Effects of Temperature and Aldehyde Fixation on Tissue Water Diffusion Properties, Studied in an Erythrocyte Ghost Tissue Model

Peter E. Thelwall,[1*] Timothy M. Shepherd,[1] Greg J. Stanisz,[2] and Stephen J. Blackband[1,3]

Ex vivo biological sample imaging can complement in vivo MRI studies. Since ex vivo studies are typically performed at room temperature, and samples are frequently preserved by fixation, it is important to understand how environmental and chemical changes dictated by ex vivo studies alter the physical and MR properties of a sample. Diffusion and relaxation time measurements were used to assess the effects of temperature change and aldehyde fixation on the biophysical and MR properties of a model biological tissue comprised of erythrocyte ghosts suspended in buffer or agarose gel. Sample temperature was varied between 10°C and 37°C. Diffusion MRI data were analyzed with a biophysically appropriate two-compartment exchange model. Temperature change resulted in a complex alteration of water diffusion properties due to the compartmental nature of tissues and alteration in membrane permeability. Formaldehyde, Karnovsky's solution, and glutaraldehyde all caused statistically significant changes to the biophysical and MR properties of the samples. Fixation caused large decreases in water proton T_2, which was restored to near prefixation values by washing free fixative from the samples. Water membrane permeability was also significantly altered by fixation. This study demonstrates that relating in vivo MR data to chemically fixed ex vivo data requires an understanding of the effects of sample preparation. Magn Reson Med 56:282–289, 2006. © 2006 Wiley-Liss, Inc.

Key words: water exchange; diffusion-weighted imaging; formaldehyde; glutaraldehyde; fixative; diffusion analysis

There has been a recent growth in the application of ex vivo MRI studies to biological tissues, organs, and entire organisms, which augment in vivo MRI by providing information that would be difficult or impossible to acquire from a living system. Ex vivo samples allow the use of stronger magnetic field gradients and permit a higher achievable signal-to-noise ratio (SNR) (also due to smaller RF coils and samples, and longer scan times) and thus higher spatial resolution, and produce data sets devoid of motion or flow artifacts. MRI of ex vivo samples has been used for morphological evaluations of human samples, particularly in neurological (1–4) and cardiac studies (5–7). A variety of animal models have been used in a similar fashion (8,9). For example, MR microscopy of fixed mice and mouse organs has been employed for morphological phenotyping (10,11), and has been widely used in diffusion tensor imaging (DTI) studies investigating the microstructure of the central nervous system (e.g., Refs. 12 and 13). Aldehyde fixation is frequently employed to preserve tissues from degradation prior to imaging, and MR data are most commonly acquired at room temperature (approximately 20°C) rather than physiological temperature (~37°C). However, it is recognized that the process of fixation may alter the morphological and physical properties of the fixed tissue, as well as the MR properties, and that these will vary with the fixative and fixation technique used (4,6,14,15). To relate data acquired from chemically fixed samples at room temperature to an in vivo situation, it is necessary to understand how these environmental and sample changes will affect the MR-visible properties of the sample. We hypothesized that diffusion MRI could be used to detect and quantify changes in tissue biophysical properties (such as membrane permeability and water diffusion rates) and MR properties (such as relaxation rates) caused by aldehyde fixation and/or changes in temperature.

The effects of fixation on biophysical and water properties of the model tissue were investigated for three fixative types. Fixatives such as formaldehyde and glutaraldehyde cross-link protein amino groups with methylene bridges to render tissues metabolically inactive and structurally stable (16). While this preserves microstructural organization within a tissue, it necessarily alters chemical and physical environments that contribute to MRI contrast mechanisms. This is significant because diffusion MRI is widely employed to image chemically fixed biological samples.

Excised tissues present a challenging system for accurate modeling of diffusion signals because of their complex and heterogeneous structure. Therefore, in this study we employed a simple biological model tissue composed of erythrocyte ghosts, a flexible system that allows independent control of its biophysical properties (17). For studies of aldehyde fixation, ghosts were immobilized in agarose gel so that samples could be immersion-fixed, analogously to the preparation of ex vivo biological samples. Since the ghosts are not metabolically active, they exhibit stable biophysical and MR properties, which is important for comparisons between fresh and chemically-fixed samples. Diffusion data were acquired from erythrocyte ghost samples at 10°C, 20°C, 30°C, and 37°C to assess the effects of

[1]Department of Neuroscience, McKnight Brain Institute, University of Florida, Gainesville, Florida, USA.

[2]Department of Medical Biophysics, University of Toronto, Imaging Research, Sunnybrook and Women's College, Health Sciences Centre, Toronto, Canada.

[3]National High Magnetic Field Laboratory, Florida State University, Tallahassee, Florida, USA.

Grant sponsor: NIH; Grant numbers: RO1 NS36992; P41 RR16105.

*Correspondence to: Peter E. Thelwall, Ph.D., Newcastle Magnetic Resonance Centre, Newcastle University, Newcastle General Hospital, Westgate Road, Newcastle upon Tyne, NE4 6BE, England. E-mail: pete.thelwall@ncl.ac.uk

Received 27 July 2005; revised 11 April 2006; accepted 12 April 2006.

DOI 10.1002/mrm.20962

Published online 13 July 2006 in Wiley InterScience (www.interscience.wiley.com).

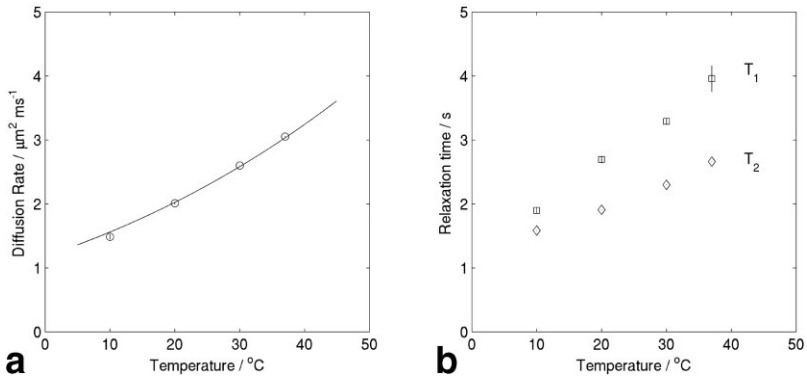

FIG. 1. **a:** The free diffusion coefficient of pure water plotted against sample temperature, measured at 10°C, 20°C, 30°C, and 37°C (○, mean of $N = 3$, standard deviation (SD) error bars within the symbols), and the published rate of water diffusion (——) as described by Mills (22). **b:** The temperature dependence of water proton T_1 (□) and T_2 (◇) in pure water (data show means ± SD, $N = 3$).

temperature on water diffusion properties in biological tissues. For the fixative studies, diffusion data were acquired from freshly prepared gel-immobilized erythrocyte ghost samples, samples that had been immersed in three types of fixative solution, and fixed samples that had been saline-washed to remove excess fixative. Additionally, the effects of a membrane water channel blocker (pCMBS) on diffusion properties were determined for all samples in the fixative study. Diffusion data acquired from this system were assessed with an analysis model appropriate to the model tissue microstructure (18), which provided information on microstructural perturbation.

MATERIALS AND METHODS

Ghost Sample Preparation

Human erythrocyte ghost samples were prepared as previously described (17), by the hypertonic lysis/gel filtration method of Wood (19). The ghost preparation method yielded a sample of resealed ghosts that were free from visible contamination with hemoglobin. Prior to MR investigation the ghosts were washed in isotonic buffered erythrocyte suspension (IBES) solution (125 mM NaCl, 5 mM HEPES, 4.5 mM KCl, 2.5 mM $CaCl_2$, 1.8 mM $MgSO_4$, 5 mM $NaHPO_4$, 10 mM glucose) and pelleted by centrifugation at 16000 × *g* for 10 min. The intracellular fraction of the pellet was determined by the degree of dilution of a fluorescently-labeled dextran solution by the extracellular space, as previously described (17).

For temperature studies the ghost suspension was diluted to an intracellular fraction of approximately 50% by the addition of IBES solution. Aliquots of this ghost suspension (80 μl, three samples per temperature group) were placed in NMR tubes (2.4 mm ID) and stored at 4°C until required for MR investigation (no more than 12 hr). To test whether sample temperature altered intracellular fraction in red blood cells, aliquots of a suspension of erythrocytes in IBES solution at approximately 60% intracellular fraction were incubated at 4°C and 37°C for 20 min (three samples per temperature group). The intracellular fraction of these samples was determined by centrifugation (10 min at 2500 × *g*) at 4°C and 37°C.

Ghost Sample Fixation

For aldehyde fixation studies the ghosts were immobilized in agarose by mixing three volumes of ghost suspension with two volumes of IBES solution containing low-melting-point agarose (1.25% w/v) at 37°C. This produced an erythrocyte suspension with an intracellular fraction of approximately 50% and 1% agarose in the extracellular space. The suspension was then placed in a 2.4-mm internal diameter glass NMR tube and cooled to 2°C. Once the agarose solution had gelled, the immobilized ghost preparation was extruded from the glass tube and immersed in 1× phosphate-buffered saline (PBS) solution (137 mM NaCl, 2.7 mM KCl, 1.0 mM Na_2HPO_4, 1.8 mM KH_2PO_4, pH 7.4, 300 mOsm kg^{-1}). The ghost-gel sample was cut into 15-mm-long samples (approximately 80 μl volume) and either stored at 4°C until required for MR investigation (no more than 12 hr (freshly prepared ghosts)) or immersed in fixative solution. The three fixative solutions used were PBS (pH 7.4, 300 mOsm kg^{-1}) containing either 4% formaldehyde, a mixture of 2% formaldehyde and 2% glutaraldehyde (Karnovsky's solution), or 4% glutaraldehyde. MR data were acquired from ghost samples after 4 weeks of immersion-fixation, both from fixative-equilibrated samples and samples that had been washed for 12 hr in 1 × PBS to remove free fixative. Washing involved placing the sample in a PBS solution with volume greater than 100× that of the sample, and exchanging PBS solutions at 30 min, 1 hr, and 11 hr after the start of washing. All MR data were acquired from triplicate samples of gel-immobilized ghosts.

After acquisition of MR data the ghost-gel samples were immersed for 1 hr in a solution containing para-chloromercuriphenylbenzene sulphonate (pCMBS), a water membrane channel blocker, to assess the effects of fixation on channel-mediated membrane water permeability. Freshly prepared and fixed-washed samples were immersed in PBS containing pCMBS (2 mM), and fixed samples were immersed in their respective fixative solution containing pCMBS (2 mM).

MR Data Acquisition

All MR data were acquired using an Oxford Instruments (Abingdon, UK) 14.1-T vertical standard bore magnet interfaced to a Bruker (Billerica, MA, USA) 600-MHz spectrometer equipped with triple-axis 3000 mT m^{-1} gradients. The temperature was controlled using a Bruker variable temperature system employing an air heater and thermocouple incorporated into the microimaging probe. The temperature

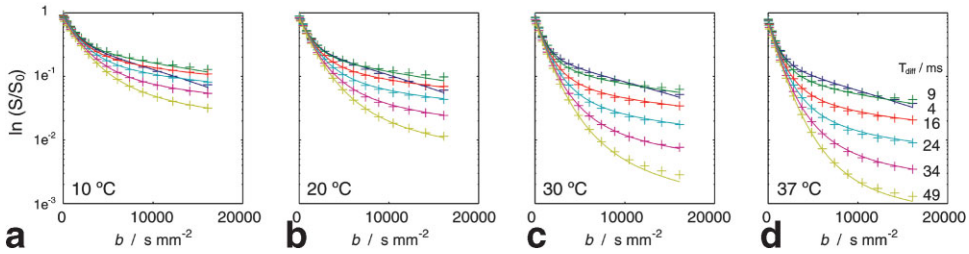

FIG. 2. Representative PGSE experiment data from a sample of erythrocyte ghosts suspended in IBES solution at temperatures of 10°C, 20°C, 30°C, and 37°C, acquired with diffusion times of 4, 9, 16, 24, 34, and 49 ms at each temperature. Sixteen of the 32 acquired data points are shown for each diffusion time (+), with two-compartment exchange model fits (——) to the data.

controller was calibrated using the chemical shifts of methanol proton resonances (20) to an accuracy of <1°C. Pulsed gradient spin-echo (PGSE) experiments (21) used gradient pulse durations (δ) of 3 ms and pulse separations (Δ) of 5, 10, 17, 25, 35, and 50 ms. Echo times (TEs) were 15, 15, 25, 30, 45, and 60 ms, respectively. Gradient strength was linearly incremented in 32 steps to produce *b*-values between 0 and 16000 s mm^{-2} for all diffusion times, and two averages were acquired per gradient increment. The repetition time (TR) for all of the PGSE experiments was 4 s, resulting in a scan time of approximately 4.5 min per diffusion measurement. T_2 relaxation times were measured with a Carr-Purcell-Meiboom-Gill (CPMG) sequence employing a TE of 4.12 ms and 256 echoes per acquisition. T_1 relaxation times were measured with an inversion-recovery sequence employing 12 logarithmically-spaced inversion times between 50 and 9000 ms. Data were acquired at sample temperatures of 10°C, 20°C, 30°C, and 37°C for the temperature study, and at 20°C for the fixation study. The total imaging time per sample was approximately 38 min. Sample temperature change was followed by a 10-min equilibration period. This period was demonstrated to be sufficient for sample temperature equilibration by measuring the chemical shifts of a methanol sample following temperature change.

Data Analysis

The PGSE data were analyzed with a two-compartment model incorporating exchange between compartments, intracellular restriction, and extracellular tortuosity, as described by Li et al. (18) and previously employed in our erythrocyte ghost studies (17). The analysis provides an index of cell size (a), extracellular apparent diffusion coefficient (ADC_{ex}, representing extracellular diffusion rate moderated by tortuosity), intracellular fraction (V_{in}), and the rate of water exchange between the intra- and extracellular compartments (k_{ie}). It should be noted that ADC_{ex} represents the *apparent* diffusion coefficient of water in the extracellular space and depends on the intrinsic free diffusion coefficient (D_{ex}), the extracellular volume fraction, and cell geometry; therefore it is always slower then D_{ex}. D_{ex} can be calculated from ADC_{ex} if the precise shape cellular shape is known (18); however, in the case of a complicated cell shape (as with the ghosts), it is difficult to precisely determine the tortuosity factor. Therefore, we report the ADC_{ex} rather than make assumptions about extracellular tortuosity.

In our previous study (17) we successfully employed this analysis to track changes in intracellular volume fraction and cell size, and demonstrated the limitations of the simpler biexponential analysis. Fits were rejected if the normalized χ^2 value was larger than 4, and acceptable fits typically had χ^2 values of approximately 0.8–1.4. A statistical comparison of ghost biophysical properties from the temperature study was performed using a one-way repeated-measures analysis of variance (ANOVA) with post-hoc Tukey multiple comparisons tests to isolate individual differences between treatment groups (SigmaStat 2.03, Point Richmond, CA, USA). A one-way ANOVA with post-hoc Tukey multiple comparisons tests was used for the fixative study. Significance for all statistical tests was defined a priori as $P < 0.05$.

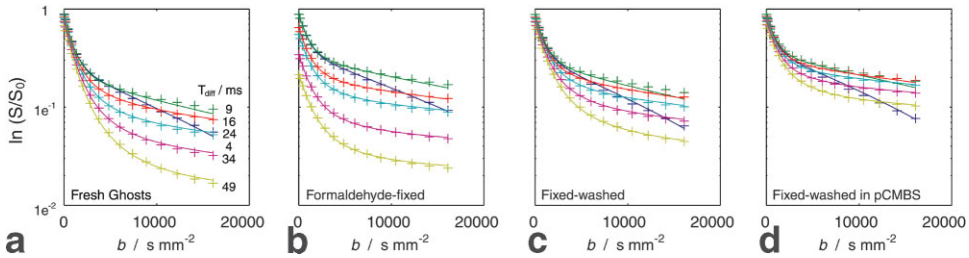

FIG. 3. Representative PGSE experiment data from a freshly prepared gel-immobilized ghost sample, a sample fixed in 4% formaldehyde, a 4% formaldehyde-fixed sample that had been PBS-washed to remove excess fixative prior to data acquisition, and the same sample after immersion in PBS containing 2 mM pCMBS. Data were acquired with diffusion times of 4, 9, 16, 24, 34, and 49 ms for each sample. Sixteen of the 32 acquired data points are shown for each diffusion time (+), with two-compartment exchange model fits (——) to the data. Plots are normalized to the $b = 0$ data point of the $T_{diff} = 4$ ms data set. The effects of reduced T_2 on the formaldehyde-equilibrated sample (**b**) are evident.

Table 1
Temperature Study: T_1 and T_2 Measurements, and Results of Two Compartment Exchange Model Fits to Diffusion Data*

Sample temperature/°C	ADC_{ex}/μm² ms⁻¹	a/μm	Mean intracellular residence time (τ)/ms	V_{in}	T_1/s	T_2/ms
10	0.94 ± 0.02[x]	2.20 ± 0.02[y]	16.8 ± 0.2[x]	0.42 ± 0.01[y]	1.90 ± 0.01[x]	334 ± 4[x]
20	1.19 ± 0.03[x]	2.09 ± 0.06	11.8 ± 0.9[x]	0.39 ± 0.02[y]	2.53 ± 0.22[x]	317 ± 3[x]
30	1.41 ± 0.01[x]	2.07 ± 0.04[z]	8.9 ± 0.1[x]	0.35 ± 0.01[y]	3.25 ± 0.05[x]	291 ± 4[x]
37	1.58 ± 0.04[x]	2.06 ± 0.05	7.1 ± 0.3[x]	0.32 ± 0.02[y]	3.86 ± 0.09[x]	271 ± 1[x]

*Data show means ± SD, $N = 3$. Fitted values that show statistically significant differences between all three[(x)], two[(y)], or one[(z)] of the other temperature measurements ($P < 0.05$) are indicated in the table.
ADC_{ex} = extracellular apparent diffusion coefficient, a = mean restriction dimension, τ = mean intracellular residence time of water molecules, V_{in} = intracellular fraction.

RESULTS

Temperature Dependence of Model Tissue Water Diffusion Properties

Figure 1a shows the free diffusion coefficient (D) of pure water plotted against sample temperature, measured at 10°C, 20°C, 30°C, and 37°C. The published rate of water diffusion determined by Mills (22) is also shown for comparison. Good agreement between experimental and literature diffusion rates was observed, confirming correct gradient strength calibration. Pure water, IBES, and PBS solutions exhibited near-identical water diffusion coefficients at each of the four temperatures (data not shown). Figure 1b shows the temperature dependence of water proton T_1 and T_2, demonstrating an increase in T_1 and T_2 with temperature.

Figure 2 shows representative PGSE data from an erythrocyte ghost sample at 10°C, 20°C, 30°C, and 37°C. Data acquired at diffusion times of 4, 9, 16, 24, 34, and 49 ms are shown for each temperature. Non-monoexponential diffusion was observed in all data sets. As observed in our previous studies, increasing the diffusion time results in decreased signal at high b-values due to the effects of compartmental exchange. Increasing the sample temperature yields an increased initial slope, decreased signal at high b-value, and greater signal attenuation at high b-value as diffusion time is increased. The two-compartment exchange model was fitted to the data to assess the biophysical origins of these diffusion changes. The results of fitting and relaxation time measurements are shown in Table 1. ADC_{ex} increased by >65% following a temperature increase from 10°C to 37°C, and the mean intracellular residence time ($\tau = 1/k_{ie}$) decreased from 16.8 to 7.1 ms. Statistically significant differences between all temperature measurements in T_1, ADC_{ex}, and mean intracellular residence time were observed ($P < 0.01$). Interestingly, a decrease in calculated V_{in} was also observed with temperature increase, with a concurrent small decrease in mean diffusion diameter (a). Also, a decrease in water proton T_2 was observed with temperature increase. To investigate the potential for a change in ghost cell dimensions, aliquots of an erythrocyte suspension were incubated at 4°C and 37°C for 20 min prior to intracellular fraction (hematocrit) measurement. The intracellular fractions were 58.1% ± 1.0% and 57.0% ± 0.7%, respectively. No significant difference between the measured intracellular fractions was observed (Student's t-test, $P > 0.05$). Thus there was no evidence of a temperature dependence for erythrocyte intracellular volume.

Effects of Sample Fixation on Model Tissue Water Diffusion Properties

The results of relaxation time and diffusion measurements from ghost-free PBS, fixative solutions, and 1% agarose gels at 20°C are shown in Table 2. The T_2 relaxation rates, R_2, of the fixative components in 1% agarose gel were 21.2, 9.8, and 10.6 s^{-1} for 4% formaldehyde, 2% formaldehyde and 2% glutaraldehyde, and 4% glutaraldehyde, respectively. Washing free fixative from the 1% agarose samples resulted in a slightly higher water proton T_2 than the prefixation T_2. Monoexponential signal attenuation was observed in T_2 and diffusion data from these control measurements.

Figure 3 shows representative PGSE experiment data from a freshly prepared gel-immobilized ghost sample, a sample fixed in 4% formaldehyde, a 4% formaldehyde-fixed sample that had been PBS-washed to remove excess fixative prior to data acquisition, and the same sample after incubation with pCMBS for 1 hr. The effects of changing membrane permeability on the PGSE experiment data can be seen as a decreasing dispersion of data acquired at different diffusion times, as clearly indicated by the differences among Fig. 3a, c, and d. The mean intracellular residence times calculated from these data were 14.1, 19.3, and 44.8 ms, respectively, for fresh ghosts, fixed-washed ghosts, and fixed-washed ghosts incubated with 2 mM pCMBS.

Table 3 shows relaxation measurements and fitted parameters of the two-compartment model for the ghost-gel data shown in Fig. 3a–c, and data from the other aldehyde-fixed samples. Fixation reduced ADC_{ex} (by approximately 7%, $P < 0.01$), but sample washing restored ADC_{ex} to near prefixation values (Table 3). The mean intracellular residence time, τ, increased for samples immersed in fixative from 14.2 ± 0.4 ms to 24–28 ms ($P < 0.01$; Table 3). Washing did not completely reverse this alteration in τ. The changes in sample T_1 and T_2 relaxation with fixation and washing mirror the relaxation rate differences of cell-free 1% agarose and cell-free 1% agarose immersed in fixative solutions. As in the temperature study, fits indicated an increase in V_{in} concurrent with mean intracellular residence time increase; however, this may not reflect a true change in intracellular volume (vide infra).

Table 4 shows fits to the samples after immersion in PBS or fixative-PBS containing 2 mM pCMBS. This membrane water channel-blocking compound reduces membrane permeability to water, and thus reduces the mean intracellular residence time, altering the effects of compartmental exchange on water diffusion properties. pCMBS caused a

Table 2
T_1, T_2, and, Apparent diffusion Coefficient Measurements from Cell Suspension Solutions and Fixative Solutions Used in the Studies*

Solution type	Sample	T_1/sec	T_2/ms	ADC/μm^2 ms^{-1}
Cell suspension solutions	Water	2.90 ± 0.02	2100 ± 10	2.03 ± 0.01
	PBS	2.82 ± 0.02	1944 ± 50	2.01 ± 0.01
	IBES	2.90 ± 0.02	854 ± 2	1.99 ± 0.01
	1% agarose in PBS	2.82 ± 0.01	173 ± 1	1.97 ± 0.01
Fixative solutions	4% formaldehyde	2.80 ± 0.01	37 ± 1[w]	1.93 ± 0.01[w]
	Karnovsky's solution	2.73 ± 0.02[w]	64 ± 2[w]	1.87 ± 0.01[w]
	4% glutaraldehyde	2.64 ± 0.01[w]	61 ± 1[w]	1.81 ± 0.01[w]
1% agarose in fixative solutions	4% Formaldehyde	2.76 ± 0.01[x]	28 ± 1[x]	1.92 ± 0.03[x,y]
	Karnovsky's solution	2.64 ± 0.01[x]	54 ± 1[x]	1.85 ± 0.01[x,y]
	4% glutaraldehyde	2.55 ± 0.01[x]	50 ± 1[x]	1.74 ± 0.01[x,y]
PBS-washed 1% agarose after immersion in fixative solution	4% formaldehyde	2.89 ± 0.01[z]	186 ± 1[z]	1.98 ± 0.01[z]
	Karnovsky's solution	2.90 ± 0.02[z]	187 ± 1[z]	1.97 ± 0.01[z]
	4% glutaraldehyde	2.91 ± 0.01[z]	178 ± 1[z]	1.98 ± 0.01[z]

*Data show means ± SD, $N = 3$, for cell-free solutions employed for cell suspension and fixation. Statistically significant differences between means ($P < 0.05$) are indicated for the fixative solutions, 1% agarose in fixative solutions, and PBS-washed 1% agarose after immersion in fixative solution.
[w]Fixative solution significantly different from PBS.
[x]Significantly different from 1% agarose in PBS.
[y]Significantly different from both other fixative-immersed 1% agarose samples.
[z]PBS-washed 1% agarose samples significantly different from the corresponding fixative-immersed sample.
ADC = apparent diffusion coefficient.

statistically significant increase in mean intracellular residence time in all samples ($P < 0.01$).

DISCUSSION

Temperature Dependence of Model Tissue Water Diffusion Properties

The temperature dependence of water diffusion in biological tissues is more complex than that of pure water due to the compartmental nature of biological tissues. Pure water diffusion rate shows a near-linear dependence on temperature over the range studied, and water diffusion in biological tissues also shows temperature dependence. Morvan and Leroy-Willig (23) demonstrated changes in muscle water ADC on exercise that they assigned in part to change in tissue temperature due to metabolic activity. Hasegawa et al. (24) demonstrated that the ADC of brain tissue water correlated with temperature in the range of 33–39°C, and suggested that in normal brain the water ADC could be used to reflect changes in brain temperature. However,

Table 3
Fixative Study: T_1 and T_2 Measurements, and Two Compartment Exchange Model Fits to Diffusion Data from Fresh, Fixed and Fixed-Washed Samples*

Sample	ADC_{ex}/μm^2 ms^{-1}	a/μm	Mean intracellular residence time (τ)/ms	V_{in}	T_1/s	T_2/ms
Freshly prepared gel-immobilized ghosts	1.38 ± 0.01	2.23 ± 0.03	14.2 ± 0.4	0.32 ± 0.01	2.63 ± 0.01	189 ± 2
4% formaldehyde-fixed	1.28 ± 0.01[w]	2.11 ± 0.03	28.0 ± 2.2[w]	0.44 ± 0.01[w,y]	2.53 ± 0.03	33.3 ± 1.4[w,y]
Karnovsky's solution-fixed	1.28 ± 0.02[w]	2.21 ± 0.04	22.9 ± 2.1[w]	0.36 ± 0.01[w]	2.42 ± 0.04	45.1 ± 0.5[w]
4% glutaraldehyde-fixed	1.20 ± 0.01[w,y]	2.21 ± 0.04	24.0 ± 0.2[w]	0.39 ± 0.01[w]	2.34 ± 0.04	49.3 ± 1.1[w]
PBS-washed after 4% formaldehyde	1.34 ± 0.05[x]	2.26 ± 0.08	21.7 ± 2.5[w]	0.41 ± 0.02[w,x,z]	2.53 ± 0.03	211 ± 3[w,x]
PBS-washed after Karnovsky's solution	1.36 ± 0.01[x]	2.24 ± 0.05	16.9 ± 0.9	0.34 ± 0.01	2.45 ± 0.06	209 ± 2[w,x]
PBS-washed after 4% glutaraldehyde	1.34 ± 0.02[x]	2.23 ± 0.06	17.1 ± 0.4[x]	0.37 ± 0.01[w]	2.46 ± 0.22	210 ± 3[w,x]

*Data show means ± SD, $N = 3$, for gel-immobilized ghost samples prior to fixation, following immersion in fixative for four weeks, and after washing in PBS. Statistically significant differences between means ($P < 0.05$) are indicated in the table.
[w]Significantly different from freshly prepared ghost samples.
[x]Washed samples significantly different from the corresponding fixative-immersed sample.
[y]Significantly different from both other fixed samples.
[z]Significantly different from both other fixed-washed samples.
ADC_{ex} = extracellular apparent diffusion coefficient, a = mean restriction dimension, τ = mean intracellular residence time of water molecules, V_{in} = intracellular fraction.

Table 4
Fixative Study: T_1 and T_2 Measurements and Two Compartment Exchange Model Fits to Diffusion Data from pCMBS-Treated Samples*

Sample	ADC_{ex}/μm^2 ms^{-1}	a/μm	Mean intracellular residence time (τ)/ms	V_{in}	T_1/s	T_2/ms
Freshly prepared gel-immobilized ghosts	1.35 ± 0.03	2.16 ± 0.03	46.3 ± 4.0[v]	0.41 ± 0.02[v]	2.63 ± 0.04	187 ± 4
4% formaldehyde-fixed	1.28 ± 0.01[w]	2.20 ± 0.05	44.8 ± 3.3[v,x]	0.44 ± 0.01[x]	2.56 ± 0.02	29.7 ± 1.1[w]
Karnovsky's solution-fixed	1.28 ± 0.01[w]	2.19 ± 0.03	37.7 ± 1.3[v,w]	0.37 ± 0.01[w]	2.46 ± 0.04	32.5 ± 0.2[w]
4% glutaraldehyde-fixed	1.22 ± 0.01[w]	2.19 ± 0.04	32.5 ± 1.4[v,w]	0.38 ± 0.01	2.34 ± 0.04	39.8 ± 0.7[w,x]
PBS-washed after 4% formaldehyde	1.33 ± 0.01	2.22 ± 0.05	42.7 ± 1.8[v,y]	0.43 ± 0.01[y]	2.56 ± 0.03	206 ± 2[w,z]
PBS-washed after Karnovsky's solution	1.41 ± 0.03[z,y]	2.29 ± 0.13	29.5 ± 4.5[v,w,z]	0.36 ± 0.02[w,y]	2.24 ± 0.29	203 ± 1[w,z]
PBS-washed after 4% glutaraldehyde	1.34 ± 0.01[z]	2.17 ± 0.01	30.8 ± 1.1[v,w]	0.39 ± 0.01[y]	2.87 ± 0.51	204 ± 3[w,z]

*Data show means ± SD, $N = 3$, for gel-immobilised ghost samples prior to fixation, following immersion in fixative for four weeks, and after washing in PBS. Statistically significant differences between means ($P < 0.05$) is indicated in the table.
[v]Significantly different from corresponding non-pCMBS-treated sample.
[w]Significantly different from freshly prepared ghost samples.
[x]Significantly different from both other fixed samples.
[y]Significantly different from both other fixed-washed samples.
[z]Washed samples significantly different from the corresponding fixative-immersed sample.
ADC_{ex} = extracellular apparent diffusion coefficient, a = mean restriction dimension, τ = mean intracellular residence time of water molecules, V_{in} = intracellular fraction.

water diffusion in biological tissues is more complex than can be described by a simple ADC measurement—hence our approach to determine the multicomponent behavior of water diffusion at a range of diffusion times, and analysis with a more biophysically appropriate model (18). Our previous studies demonstrated that water diffusion in ghosts suspensions could be well described by tortuous extracellular diffusion, restricted intracellular diffusion, and exchange of water between intra- and extracellular compartments (17). The temperature experiment analyses presented here broadly support this description, in which different water compartments show different responses to temperature change. As temperature is increased, ADC_{ex} increases but intracellular water remains diffusion-restricted by the cell membrane. This can be seen in the raw data (Fig. 2) as an increase in initial slope, but no change in slope at high *b*-values, as temperature is increased. The value of τ decreases with temperature increase, as has been well documented in other studies (25). In the raw data (Fig. 2) this is manifested as greater signal attenuation with increasing diffusion time as temperature is increased.

Sample T_1 changes significantly with temperature (Fig. 1), and one could postulate that fitted diffusion parameters could be affected by altered sample T_1. However, T_1 was a parameter in the analysis model, and diffusion experiments that employed long TRs (12 s) showed no significant differences in fitted parameters compared to fits from data acquired with a TR of 4 s (data not shown).

The observed decrease in sample T_2 with temperature increase (Table 1) was unexpected, given the temperature dependence of T_1 and the potential for T_1 to influence T_2 (Fig. 1b). Also, an unexpected decrease in calculated intracellular fraction (V_{in}) was observed with temperature increase, although independent measures of intracellular fraction temperature dependence in erythrocyte samples did not corroborate this observation. A change in V_{in} was also observed in the fixative study when membrane permeability was altered with pCMBS, or on fixation (vide infra). Since V_{in} represents the visible intracellular spin pool, it is plausible that with increased temperature an elevated water mobility results in an increased number of intracellular spins experiencing T_2 relaxation effects via membrane or protein interactions (e.g., by increased exchange with intracellular bound water). An increase in exchange with a bound water pool would decrease the fraction of visible intracellular spins, and thus reduce the calculated V_{in} and sample T_2 despite an unchanged intracellular fraction.

These studies of temperature effects on water diffusion properties demonstrate that a simple correlation of diffusion data acquired from biological tissues at different temperatures requires caution because of the complex interaction among restriction, tortuosity, and exchange effects. However, these data provide clues about how we may be able to modify and improve MR data acquisition and fitting models to properly account for temperature dependencies.

Effects of Sample Fixation on Model Tissue Water Diffusion Properties

Aldehyde chemical fixation caused major changes to the biophysical properties of the model tissue and the MR properties of tissue water. Removal of excess fixative by washing in PBS reversed some, but not all, of these changes. A dramatic decrease in sample T_2 was observed on fixation. This effect was greatest with 4% formaldehyde and least for 4% glutaraldehyde. Formaldehyde and glutaraldehyde form hydrates in aqueous solution that crosslink a portion of the water into a polymeric matrix (16,26), slowing molecular motion and reducing water ADC and proton T_2. Bossart et al. (27) demonstrated that washing

free fixative from samples lengthens water proton T_2; our data confirm this observation and show that washing elevates water proton T_2 beyond prefixation values. However, this may be due to a change in the relaxation properties of agarose in the extracellular space, since a similar effect was seen in cell-free agarose control samples (Table 2). Whether it originates from the agarose or the ghost cells, the elevation of T_2 above prefixation values in fixed-washed samples is presumably due to a permanent alteration of model tissue components that contribute to water proton T_2, which results from chemical changes that are not reversed by washing free fixative from the sample.

Fixation also significantly altered membrane permeability. These changes were not completely reversed after the free fixative was washed away. Transmembrane water exchange occurs via both channel-mediated and nonspecific pathways, including passage through transmembrane protein channels (both aquaporins and channels associated with transport of other molecules, such as glucose) and water diffusion through the lipid bilayer (25,28). In our experiments we attempted to determine whether the fixation-induced changes in membrane permeability originate from alterations in channel-mediated or lipid bilayer permeabilities to water. We hypothesized that if fixation reduced membrane permeability by disrupting aquaporin channels, then the effects of channel blockers such as pCMBS would be minimal in those fixed samples, since the water passage through the channels would already be disrupted. However, if fixatives leave aquaporin function unaffected but alter lipid bilayer permeability to water, the addition of pCMBS would reduce membrane water permeability in fixed samples to a lower permeability than observed for unfixed ghosts incubated with pCMBS.

The results of this study (Tables 3 and 4) show that pCMBS increased the mean intracellular residence time from approximately 14 ms to 46 ms in fresh ghosts. Fixed ghosts had residence times of 23–28 ms, with 4% formaldehyde showing the largest decrease in membrane permeability. The addition of pCMBS to fixed samples further increased residence times. The 4% formaldehyde-fixed pCMBS-treated sample had a residence time equal to (but not greater than) that of nonfixed ghosts in pCMBS. This supports the hypothesis that fixative interaction with aquaporin channels causes an alteration in membrane water permeability. Interestingly, pCMBS has less of an effect on samples fixed in 4% glutaraldehyde or 2% formaldehyde, 2% glutaraldehyde. One could propose that this may be due to pCMBS reacting with free fixative rather than blocking membrane channels, yet the same effect is observed in ghost samples that had been washed of free fixative. This suggests that glutaraldehyde-containing fixatives may alter membrane channels in a manner that reduces the channel-blocking ability of pCMBS. The membrane permeability changes observed on fixation were reversed to some extent when free fixative was washed from the samples. The 4% formaldehyde had the greatest residual effect on membrane permeability after washing. Thus one might choose a particular aldehyde fixative solution to minimize perturbation of membrane permeability if this biophysical property is considered most relevant to the MR measurement.

Similarly to the temperature experiments, unexpected changes in V_{in} were observed between different sample groups in the fixative experiments. Further studies are required to investigate whether the intracellular fraction changed on fixation and/or pCMBS treatment, or whether the changes in V_{in} represent an alteration in the visible spin population but not a change in physical dimensions of the cells. Although fixative buffer solutions have the potential to alter cell volume, the fixatives used in this study were suspended in isotonic (300 mOsm/kg) PBS, and studies have indicated that the fixative components of the solution do not contribute to the osmotic potential (16).

The data show that significant changes in both tissue biophysical properties and tissue water MR properties occur with temperature change or aldehyde fixation. This is highly significant for comparisons of data acquired under in vivo and ex vivo conditions. Sun et al. (29,30) suggested that similar DTI data could be acquired from in vivo and ex vivo rat brain measurements (measured in both healthy (29) and infarcted (30) brain); however, in their studies different *b*-value ranges and diffusion times were used for comparisons of fixed and live sample MRI data. Nonetheless, the importance and relevance of employing ex vivo studies to noninvasively investigate brain structure and function is clear. The studies reported here focus on relating in vivo and ex vivo data sets by demonstrating the relative contributions of biology and sample preparation to the MR data.

CONCLUSIONS

We have employed a simple model of biological tissues to characterize how sample temperature and aldehyde fixation alter the diffusion properties of tissue water. This is significant because an increasing number of studies are being performed on chemically-fixed ex vivo tissue samples, and an understanding of the biophysical and MR changes associated with temperature change and fixation are required to relate ex vivo data to the in vivo situation. Temperature change and aldehyde fixation altered both the MR properties of tissue water and the biophysical properties of the model tissue. Temperature increase resulted in an increase in the ADC of extracellular water, and an increase in water exchange between the tortuous extracellular compartment and the diffusion-restricted intracellular compartment. An unexpected decrease in water proton T_2 was also observed with temperature increase.

The formaldehyde and glutaraldehyde-based fixative solutions greatly reduced sample T_2 and slightly reduced extracellular water ADC. Washing free fixative from samples restored ADC_{ex} to prefixation values and increased water proton T_2 to longer than prefixation values; however, this may be attributable to the effect of fixative on agarose in the extracellular component. The fixatives also reduced membrane permeability to water, and this effect was partially reversed on sample washing.

Erythrocyte ghosts represent a very simple model system that is well suited to monitoring changes in the MR and biophysical properties of a tissue upon environmental change, and avoids the confounding biological interactions that can hinder in vivo studies. We extended this

model to viable ex vivo brain slices (31) and obtained a tissue model that is more representative of the in vivo situation. Our studies demonstrate that an understanding of the effects of sample preparation is essential to correctly interpret MR data acquired from chemically fixed biological samples.

ACKNOWLEDGMENTS

The authors thank Dan Plant for technical assistance, and Harm Knot for the use of his osmometer.

REFERENCES

1. Hirsch WL, Kemp SS, Martinez AJ, Curtin H, Latchaw RE, Wolf G. Anatomy of the brainstem: correlation of *in vitro* MR images with histologic sections. AJNR Am J Neuroradiol 1989;10:923–928.
2. Fatterpekar GM, Naidich TP, Delman BN, Aguinaldo JG, Gultekin SH, Sherwood CC, Hof PR, Drayer BP, Fayad ZA. Cytoarchitecture of the human cerebral cortex: MR microscopy of excised specimens at 9.4 Tesla. AJNR Am J Neuroradiol 2002;23:1313–1321.
3. Padgett KR, Maria BL, Yachnis AT, Blackband SJ. *Ex vivo* high-resolution magnetic resonance imaging of the brain in Joubert's syndrome. J Child Neurol 2002;17:911–913.
4. Pfefferbaum A, Sullivan EV, Adalsteinsson E, Garrick T, Harper C. Postmortem MR imaging of formalin-fixed human brain. Neuroimage 2004;21:1585–1595.
5. Hsu JC, Johnson GA, Smith WM, Reimer KA, Ideker RE. Magnetic resonance imaging of chronic myocardial infarcts in formalin-fixed human autopsy hearts. Circulation 1994;89:2133–2140.
6. Dalager-Pedersen S, Falk E, Ringgaard S, Kristensen IB, Pedersen EM. Effects of temperature and histopathologic preparation on the size and morphology of atherosclerotic carotid arteries as imaged by MRI. J Magn Reson Imaging 1999;10:876–885.
7. Holmes AA, Scollan DF, Winslow RL. Direct histological validation of diffusion tensor MRI in formaldehyde-fixed myocardium. Magn Reson Med 2000;44:157–161.
8. Benveniste H, Blackband S. MR microscopy and high resolution small animal MRI: applications in neuroscience research. Prog Neurobiol 2002;67:393–420.
9. Benveniste H, Mareci TH, Blackband SJ. Anatomical studies in the rodent brain and spinal cord: applications of magnetic resonance microscopy. In: van Bruggen N, Roberts T, editors. Techniques of biomedical imaging in neuroscience. Boca Raton: CRC Press, 2003. p 211–235
10. Johnson GA, Cofer GP, Fubara B, Gewalt SL, Hedlund LW, Maronpot RR. Magnetic resonance histology for morphologic phenotyping. J Magn Reson Imaging 2002;16:423–429.
11. Johnson GA, Cofer GP, Gewalt SL, Hedlund LW. Morphologic phenotyping with MR microscopy: the visible mouse. Radiology 2002;222:789–793.
12. Zhang J, Richards LJ, Yarowsky P, Huang H, van Zijl PC, Mori S. Three-dimensional anatomical characterization of the developing mouse brain by diffusion tensor microimaging. Neuroimage 2003;20:1639–1648.
13. Zhang J, Chen YB, Hardwick JM, Miller MI, Plachez C, Richards LJ, Yarowsky P, van Zijl P, Mori S. Magnetic resonance diffusion tensor microimaging reveals a role for Bcl-x in brain development and homeostasis. J Neurosci 2005;25:1881–1888.
14. Tovi M, Ericsson A. Measurements of T1 and T2 over time in formalin-fixed human whole-brain specimens. Acta Radiol 1992;33:400–404.
15. Thelwall PE, Shepherd TM, Stanisz GJ, Blackband SJ. Effect of fixative osmolality on biological tissue microstructure studied with an erythrocyte ghost model. In: Proceedings of the 12th Annual Meeting of ISMRM, Kyoto, Japan, 2004. p 1233.
16. Kiernan JA. Histological and histochemical methods: theory and practice. Oxford: Butterworth-Heinemann; 1999. 502 p.
17. Thelwall PE, Grant SC, Stanisz GJ, Blackband SJ. Human erythrocyte ghosts: Exploring the origins of multiexponential water diffusion in a model biological tissue with magnetic resonance. Magn Reson Med 2002;48:649–657.
18. Li JG, Stanisz GJ, Henkelman RM. Integrated analysis of diffusion and relaxation of water in blood. Magn Reson Med 1998;40:79–88.
19. Wood PG. Preparation of white resealable erythrocyte ghosts. Methods Enzymol 1987;149:271–280.
20. Van Geet AL. Calibration of the methanol and glycol nuclear magnetic resonance thermometers with a static thermistor probe. Anal Chem 1968;40:2227–2229.
21. Stejskal EO, Tanner JE. Spin diffusion measurements: spin echos in the presence of a time-dependent field gradient. J Chem Phys 1965;42:3597–3603.
22. Mills R. Self-diffusion in normal and heavy water in the range 1–45 C. J Phys Chem 1973;77:685–688.
23. Morvan D, Leroy-Willig A. Simultaneous measurements of diffusion and transverse relaxation in exercising skeletal muscle. Magn Reson Imaging 1995;13:943–948.
24. Hasegawa Y, Latour LL, Sotak CH, Dardzinski BJ, Fisher M. Temperature dependent change of apparent diffusion coefficient of water in normal and ischemic brain of rats. J Cereb Blood Flow Metab 1994;14:383–390.
25. Benga G, Pop VI, Popescu O, Borza V. On measuring the diffusional water permeability of human red blood cells and ghosts by nuclear magnetic resonance. J Biochem Biophys Methods 1990;21:87–102.
26. Hahnenstein I, Albert M, Hasse H, Kreiter C, Maurer G. NMR spectroscopic and densimetric study of reaction-kinetics of formaldehyde polymer formation in water, deuterium-oxide, and methanol. Indust Eng Chem Res 1995;34:440–450.
27. Bossart EL, Inglis BA, Silver XS, Mareci TH. The effect of fixative solutions in magnetic resonance imaging. In: Proceedings of the 7th Annual Meeting of ISMRM, Philadelphia, PA, USA, 1999. p 1928.
28. Zeuthen T. How water molecules pass through aquaporins. Trends Biochem Sci 2001;26:77–79.
29. Sun SW, Neil JJ, Song SK. Relative indices of water diffusion anisotropy are equivalent in live and formalin-fixed mouse brains. Magn Reson Med 2003;50:743–748.
30. Sun SW, Neil JJ, Liang HF, He YY, Schmidt RE, Hsu CY, Song SK. Formalin fixation alters water diffusion coefficient magnitude but not anisotropy in infarcted brain. Magn Reson Med 2005;53:1447–1451.
31. Shepherd TM, Thelwall PE, Stanisz GJ, Blackband SJ. Chemical fixation alters the water microenvironment in rat cortical brain slices—implications for MRI contrast mechanisms. In: Proceedings of the 13th Annual Meeting of ISMRM, Miami, FL, USA. 2005. p 619.